Copper ion Adsorption In Waste Water Using Silver Metal Nanocomposite From Avocado Pear Seed

ABSTRACT

This study investigates the adsorption potential of silver nanocomposite synthesized from avocado pear seed for the removal of copper (II) ions from aqueous solutions. The agro waste underwent treatment processes such as chemical, physical and hydrothermal synthesis giving rise to a nanocomposite with an enhanced surface area, structure and functional groups. In the investigation of the adsorption capacity of copper (II) ions, numerous factors were examined, including pH, concentration, dose, temperature, and contact time.Atomic Absorption Spectroscopy (AAS) was used to investigate the equilibrium kinetics and thermodynamics for the adsorption. The ability of copper ion uptake by the nanocomposite was examined under the characterization study of FTIR, SEM, and XRD. Langmuir and Freundlich adsorption models were employed to the experimental data and the goodness of their fit for adsorption was compared. It was determined that the Langmuir adsorption model provided a better fit compared to the Freundlich model.

Keywords: Adsorption, Avocado peer seed (APS), Copper, Silver metal nanocomposite(AgAPS)

1.0 INTRODUCTION

Nanotechnology is the scientific manipulation of matter at the molecular level that makes it possible to create materials with special qualities and uses. Nanotechnology, which first appeared at the turn of the century, has transformed material science and engineering and produced ground-breaking discoveries. The creation of materials at the nanoscale, usually smaller than 100 nm, with unique physical and chemical properties is a crucial use of nanotechnology [1]. The unique optoelectronic properties of metal nanoparticles, which are made solely from metal precursors, are also influenced by localized surface plasmon resonance (LSPR). Notably, the production of noble metals such as gold (Au) and silver (Ag) has been thoroughly studied due to its controllable size, shape, and facet, which is essential for advanced material applications [2]. According to [3] nanoparticles, a specific category of nanomaterials, have garnered significant attention in contemporary research across several industries due to their distinctive characteristics and extensive array of potential uses. Nanoparticles are preferred over alternative adsorbents because of the possession of numerous sorption sites, substantial specific surface area, capacity for low-temperature modification, porosity, surface functionalities, limited intraparticle diffusion distance, and ability to bind ions [4]. The utilisation of plant extract in green nanotechnology presents a

promising avenue for the creation of innovative nanoparticles possessing the necessary attributes for the advancement of biotechnology [5].Avocado pear or alligator pear are the names given to the fruit produced by the avocado plant (Perseaamericana), which belongs to the Lauraceae family. The seeds of avocado pears, a byproduct of the fruit, have been used medicinally to treat conditions such as diabetes, cancer, inflammation, and high blood pressure ([6]; [7]; [8]). In Ojoto and neighboring Igbo-speaking communities in southeast Nigeria, the fruit is locally known as ubeoyibo, translating to "foreign pear" [9]. Traditional medicine practices in these regions have utilized avocado pear for its antibacterial properties [10].

However, Over the course of several decades, heavy metals have emerged as significant contributors to water contamination [11]. Industrial production can result in the emission of a range of harmful compounds, including both organic and inorganic molecules, as well as toxic solvents and volatile organic chemicals. If these waste materials are discharged into aquatic ecosystems without sufficient treatment, they will result in the contamination of water bodies [12].

Heavy metal pollution in the environment has been greatly exacerbated by mining operations, agricultural practices, and fast industrialization [13]. Through metallurgical and electroplating processes, these pollutants which include heavy metals like copper (Cu(II)), cadmium (Cd(II)), and lead (Pb(II)) are released into water bodies, contaminating sources of drinking water and causing major health concerns to both humans and the environment [14]. For example, chronic exposure to Cu(II) has been associated with its bioaccumulation in foods such mushrooms, liver, mussels, and nuts. Adsorption has become one of the most successful and economical wastewater treatment techniques for reducing the negative impacts of heavy metal contamination. Cu(II) and other heavy metals may be effectively removed from aqueous solutions using biomass-based adsorbents and nanomaterials [15]. Though successful in adsorption, conventional techniques such chemical precipitation, membrane separation, ion exchange, and electrolysis are frequently costly, inefficient for large-scale applications, or non-biodegradable [16]. On the other hand, nanotechnology provides environmentally friendly and reasonably priced substitutes via processes like chemical reduction, photoreduction, and thermal breakdown [17,18]. The need for creative solutions is highlighted by the fact that these pollutants lower agricultural output, have an impact on food security, impact negatively on health and cause financial losses. Therefore removal of heavy metal ions in effluents remains imperative to mitigate the above problems as this research aims at addressing the challenges of heavy metal contamination by investigating the adsorptive removal of Cu(II) ions from aqueous solutions using a biosynthesized nanocomposite. Specifically, silver nanocomposites will be synthesized using avocado peer seed. The biosynthesized nanocomposites will be characterized to elucidate their structural and functional properties. Equilibrium, kinetic, and thermodynamic studies will be conducted to assess the adsorption efficiency, with adsorption mechanisms analyzed through Langmuir and Freundlich isotherm models.

2.0 Methodology

2.1 Preparation of the agro waste

The avocado pear seed was collected from Achina, in Aguata L.G.A of Anambra State. Nigeria. They were washed with distilled water, allowed to dry away from direct sunlight and ground into powder, then subjected to a 48-hour extraction process at room temperature using methanol as the solvent. Subsequently, the extracts utilizing Whatman No.1 paper, resulted in an extraction of crude extracts subsequent to concentration under reduced pressure.

2.2 Synthesis of Silver Nano Composites

1M $AgNO_3$ solution was prepared by simply dissolving $AgNO_3$ flakes with distilled water. Samples of the avocado pear seed extract were added to the $AgNO_3$ solution. The combination was subjected to incubation at ambient temperature until the yellow hue of the solution transitioned to a deep brown shade. The samples were then centrifuged for 20 minutes at 11000 revolutions per minute, and the supernatant was disposed of after the process. A volume of 5 mL of deionized water was introduced to the precipitate, followed by another round of centrifugation under identical conditions. The procedure was replicated. Subsequently, the ultimate precipitate was subjected to a temperature of 60°C in a hot air oven for a duration of 30 minutes.

2.3 Preparation of Stock Solutions (Adsorbate)

Distilled water was used throughout the experiment to dilute copper chloride dehydrate (≥ 99% purity) obtained from the chemical shop. All solutions used in the experiment were prepared in double distilled water. Stock solution of the test reagent of 1000mg/L was prepared by dissolving 1 gram of copper chloride dehydrate(≥ 99% purity) in 1 liter of distilled water. The stock solution underwent dilution in order to get various quantities of copper ions that were necessary for conducting the tests.

2.4. Characterization of Adsorbents

2.4.1. Fourier Transform InfraRed Spectroscopy (FTIR)

The Fourier Transform InfraRed (FTIR) Spectrophotometer was employed to ascertain the functional groups present in the samples

2.4.2. Scanning Electron Microscope (SEM) Analysis

SEM was used to ascertain the structural characteristics of the nanocomposite acquired. The dried samples were affixed to a sample holder using double conductive tape at room temperature. To enhance conductivity, a layer of platinum-gold coating was administered onto the samples. Subsequently, the samples were subjected to visualization using an 80 kV voltage.

2.4.3. X-ray Diffraction (XRD) Analysis

X-ray diffraction (XRD) was employed to analyse the crystalline nature of the AgNPs. The experiment employed a powdered material, and the scanning mode was conducted using a current of 30 mA, a voltage of 40 kV, and Cu/Kα radiation. The diffraction pattern was then recorded within the 2θ angle range of 20^0C–70^0C.

The scherrer equation was used to determine the particle size and is giving by

$$D = \frac{K\lambda}{\beta Cos\theta} \quad 2.1$$

Where D is the nanocomposite crystalline size, K represents the Scherrer constant (0.98), λ denotes the wavelength(1.54), β denotes the full width at half maximum (FWHM).

2.5. Batch Adsorption process

The batch experiments were performed using adsorbent material placed in Erlenmeyer flasks, which were sealed with glass stoppers to minimize evaporation. The mixtures were stirred using a mechanical magnetic stirrer operating at a speed of 200 revolutions per minute. The objective was to determine the optimal conditions in terms of pH, adsorbent type, and lead(II) ion concentrations.

2.5.1. Effect of pH

In order to determine the effect of pH on the adsorption of copper(II) ions onto Avocado pear silver nanocomposite, the adsorption mixture was brought into equilibrium with a 20 ml solution containing 150 mg/dm^{-3} of copper(II) ions and dried adsorbent. The experiment was conducted at pH levels of 2, 4, 6, 8, and 10. The pH was adjusted by employing 0.1 M hydrochloric acid (HCl) and 0.1 M sodium hydroxide (NaOH) solutions. The experiment involved the regulation of the adsorbent quantity to 0.1g, the temperature to 30^0C, and the duration to 60 minutes.

2.5.2. Effect of adsorbent dosage

The impact of adsorbent dose was investigated by manipulating the weights of the Nano composites within the range of 0.1g, 0.2g, 0.3g, 0.4g, and 0.5g. Subsequently, these samples were subjected to testing under the specified experimental circumstances. The experimental conditions included a duration of 60 minutes, a temperature of 300°C, a pH value of 6, and a concentration of 150 mg/L.

2.5.3. Effect of time

The study investigated the impact of time by manipulating the duration at intervals of 30 minutes, namely at 30, 60, 90, 120, 150, and 180 minutes. These variations were examined under the specified experimental settings. The experimental conditions included a temperature of 300°C, a pH value of 6, a dosage of 0.1g, and a concentration of 150 mg/L.

2.5.5. Effect of Temperature

The study investigated the impact of temperature by manipulating the duration at intervals of 5^oC, namely at 30, 35, 40, 45 and 50^OC. These variations were examined under the specified experimental settings. The experimental conditions included a pH value of 6, a dosage of 0.1g, and a concentration of 150 mg/L.

2.5.6. Effect of initial metal ion concentration

The impact of the initial metal ion concentration was investigated by manipulating concentrations at 100 mg/L, 150 mg/L, 200 mg/L, 250 mg/L, and 300 mg/L under the specified experimental settings. The experimental conditions included a time duration of 60 minutes, a dosage of 0.1g, a temperature of 300°C, and a pH level of 6.The metal solutions' concentrations were determined using atomic absorption spectroscopy, specifically utilizing the AA500F Atomic absorption spectrophotometer. Additionally, a

control experiment was conducted utilizing identical solution and equipment, with the exception of the nano-composite adsorbents.

2.5.5. Adsorption Capacity

The experimental adsorption capacity (qe mg/g) after equilibrium was calculated as follows:

$$q_{e=(C_0 - C_e)\frac{V}{m}} \quad 2.2$$

Where Co and Ce are the initial and equilibrium concentration (mg/L) of Pb respectively. "V" is the volume of the solution and "m" is the amount of adsorbent.

$$E\% = \frac{(C_0 - C_e)}{C_0} x\ 100 \quad 2.3$$

Where E is the Adsorption capacity.

2.6 Kinetic Studies

The kinetic studies was carried out with different concentrations (10mg L^{-1} , 20mg L^{-1}, 30mg L^{-1}) of solutions at room temperature (300K) in contact with the optimum dosage prepared nanoparticle (adsorbent). Samples of Cu(II) were removed at different time intervals (20 to 100min) and the metal concentration was measured. The metal uptake was calculated using kinetic equations. The sorption kinetic data of Cu(II) on the adsorbent was analysed in terms of pseudo first order and pseudo second order sorption equations. The pseudo first order equation was first suggested by Lagergren and the equation is below.

2.7 Equilibrium Isotherm Models

Investigating the adsorption isotherm, two models were used. The Langmuir and the Freundlich.

Isotherm plots were drawn from the experimental data of the amount of Cu(II) adsorbed per unit mass (mg g^{-1}) versus equilibrium solution concentration for the adsorption of Cu(II).

2.8 Thermodynamic studies

Thermodynamic equations were employed to determine the spontaneity of adsorption and to investigate the impact of temperature on the adsorption process. The calculation of the equilibrium constant, Kc, relies on equation (2.5). Consequently, the thermodynamic equation can be expressed in a linear form, known as the van't Hoff isotherm equation, as depicted in equation 2.4.

$$\Delta G = -RTlnk_C \quad 2.4$$

$$lnk_C = \left(\frac{C_A}{C_e}\right) \quad 2.5$$

$$lnk_C = \left(\frac{-\Delta H}{R}\right).\frac{1}{T} + \left(\frac{\Delta S}{R}\right) \quad 2.6$$

3.0 RESULTS AND DISCUSSION

3.1 Infrared Spectroscopic Studies

Infrared Spectroscopic Studies for avocado pear seed (APS) and Silver Oxide nano-particle-Avocado Pear Seed (AgAPS)

The FTIR spectrum of APS and AgAPS and the observed signals are presented below:

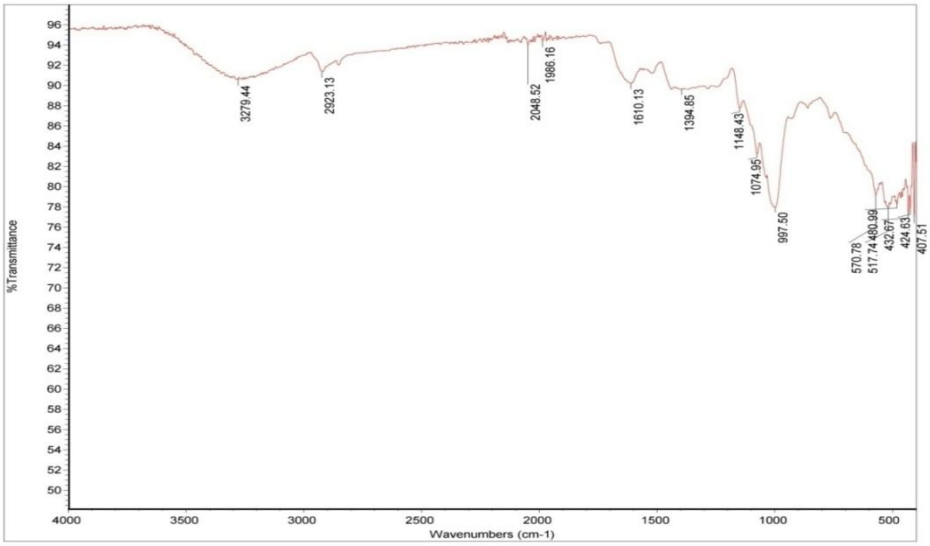

Fig 1. Infrared Spectroscopic Spectrum for avocado pear seed (APS)

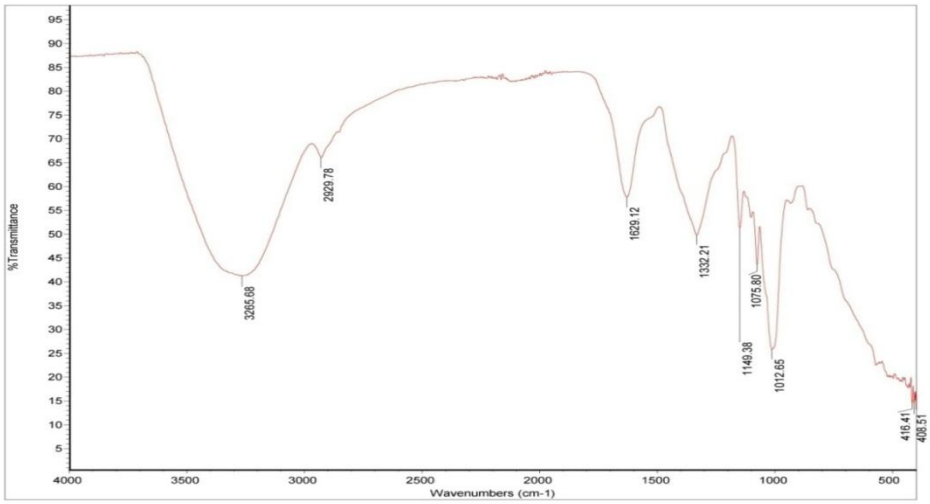

Fig 2. Infrared Spectroscopic Spectrum of Silver Oxide nano-particle-Avocado Pear Seed (AgAPS)

Table 1. Assignments of the IR spectra bands of functional groups in APS and AgAPS

APS band positions (cm^{-1})	AgAPS band positions (cm^{-1})	Proposed signal group
3279	3265	OH stretching
2923	2929	CH stretching
2048 and 1986	-	C≡C of alkynes
1610	1629	C=O stretching
1394	1332	C-H bending
1148	1149	C-O stretching
1074	1076	C-O stretching

After impregnation of silver oxide nano-particles (AgNOPs) onto APS, shifts were observed in the absorption bands of the OH group from 3279 to 3265cm-1, the C-H bands from 2923 to 2929 cm-1, the C=O bands from 1610 to 1629cm-1, the C≡C bands completely disappeared. This shows the interaction of the impregnated AgONPs with the surface functional groups on the APS surface. In addition, the presence of surface functional group on both the APS and AgAPS sorbents, indicates the potential of the prepared sorbents to remove pollutants from aqueous medium. This is in agreement with[19].

3.2 XRD Characterization

XRD Spectroscopic Studies for avocado pear seed (APS) and Silver Oxide nano-particle-Avocado Pear Seed (AgAPS)

The XRD spectra provides information on the crystal phase of the Sorbents as shown in Figure 3 for APS, the cellulose diffraction at 2θ of 15^0, 17^0, 27^0 and 31^0 is characteristics of agrowaste[20]. For AgAPS as shown in Figure .4, the face centred cubic structure of Ag nanoparticle was confirmed by 2θ diffractions at 38^0, 44^0, 65^0 and78^0 corresponding to (111), (200), (220) and (311) Ag reflections respectively. This proves the presence of similar nanoparticles on the AgAPS composites. Similar diffractions were obtained for Ag nanoparticles synthesized from the seed extract of Alpina Kat Sumodai as reported by[21].

The scherrer equation was employed in figure 4 to determine the particle size of the higher peaks in the spectra. The 2θ diffractions at the 5 highest peak, 15^o, 17^0, 39^0, 65^0 and 78^0 has an average particle size of 95nm

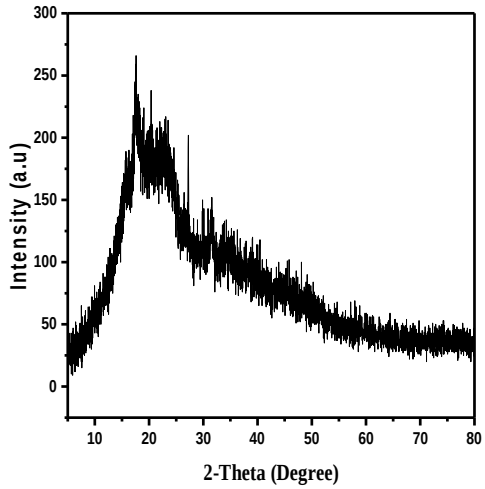

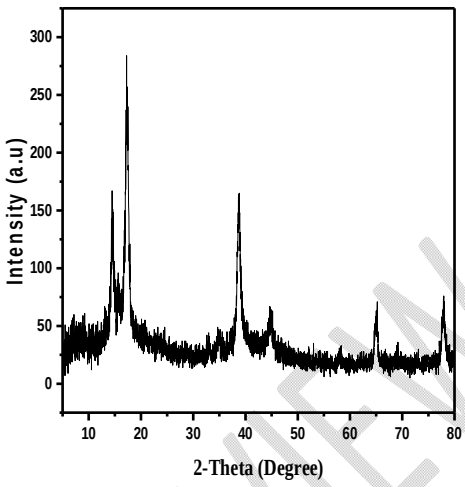

Fig3. XRD Spectroscopic Spectrum for avocado pear seed (APS)Fig 4. XRD Spectroscopic Spectrum for Silver Oxide nano-particle-Avocado Pear Seed (AgAPS)

3.3 SEM Charaterization

Scanning electron microscopy (SEM) was used to examine the surface morphology of the produced silver oxide nanocomposites at various magnifications. In contrast to avocado pear biomass, which is sparse and not as diagonally formed as those of AgAPS, the avocado pear seed nanocomposite (AgAPS) has similar rough surfaces, irregular surface structure, and hexagonal shape. The pictures show how the aggregation form of the silver oxide composite is forming an uneven surface structure. Zinc oxide nanoparticles made from CostusAfers leaf extract produced similar spectra [22].

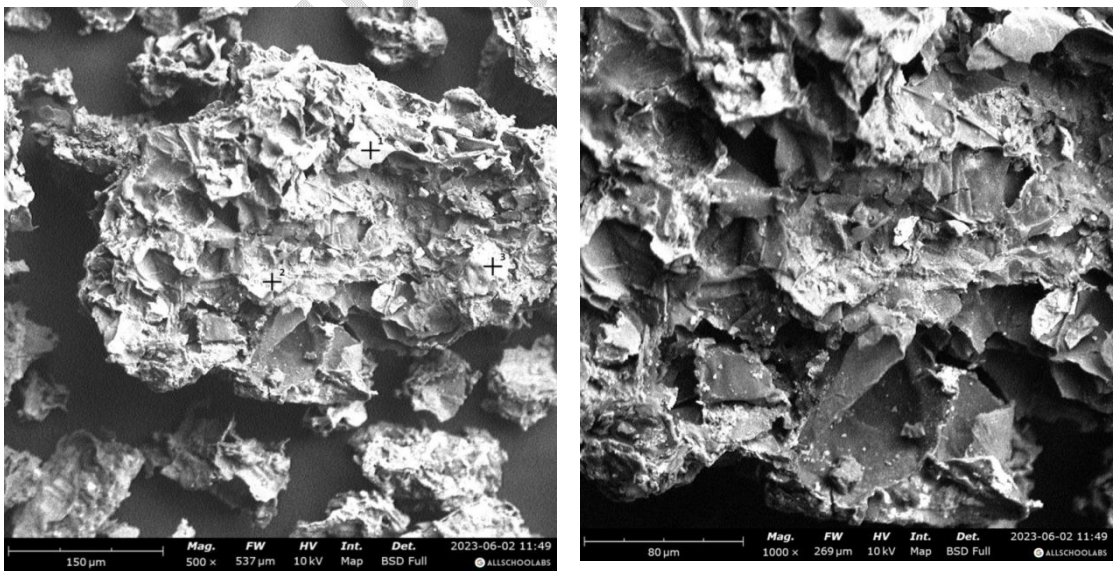

Fig 5(A-B). SEM **Spectrum of 500 and 1000 Mag for Silver Oxide nano-particle-Avocado Pear Seed (AgAPS)**

3.4 Effect of Time on Adsorption of Copper onto Avocado Pear Seed

Figure below displays the findings of the investigation into the impact of time on the adsorption of copper onto avocado pear seed (APS) and silver nanocomposite (AgAPS). The proportion of copper removed rose when the sorption duration increased from 30 to 180 minutes. The maximal adsorption capacity of the AgAPS was 29.3966 mg/g, and the APS was 28.1994 mg/g after 180 minutes. According to[23], the first rapid adsorption may have resulted from the material's surface adsorption followed by penetration into the inner tiny gaps. According to[24], the attachment-controlled process that results from a decrease in the number of sites available for active adsorption may be the source of the sluggish adsorption rate over time.The results showed the fast and stable nature of the process as only an insignificant difference was observed between the initial and final contact time[25]. In all the time studied, AgAPS showed a higher adsorption capacity than APS. This might be due to enhanced active adsorption sites created by the presence of Ag molecules. The results obtained in this study are in agreements with reports elsewhere[26].

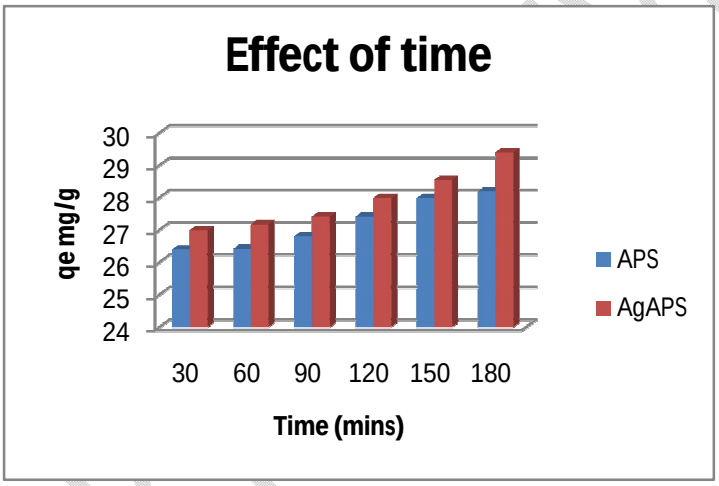

Figure 6. Effect of time on the adsorption of copper onto avocado pear seed

3.5 Effect of pH on the adsorption of copper onto avocado pear seed

In any adsorption investigation, the adsorbent and adsorbate species are impacted by the waste water's solution pH. This results in changes to the surface charge and speciation at different pH levels due to the protonation or deprotonation of the functional groups in both the adsorbent and the adsorbate[26]. During the adsorption process, charged species may come into contact with one another via electrostatic interactions. As a result, solution pH is a crucial factor that influences adsorption and should be taken into account. The figure below displays the findings of the pH's impacts on copper's adsorption onto APS and AgAPS. The equilibrium sorption capacity was minimum at pH 2 (24.7965 and 24.8874mg/g) for APS and AgAPS respectively and reached a maximum at pH 10 (27.6342mg/g) for APS and pH 10 (28.1215mg/g) for AgAPS. The lower sorption capacity at low pH can be explained by the fact that at acidic pH, H^+ may compete with Cu^{2+} ions for the adsorption sites of the adsorbent, thereby inhibiting the adsorption of copper ions. Similar results are reported by [27].

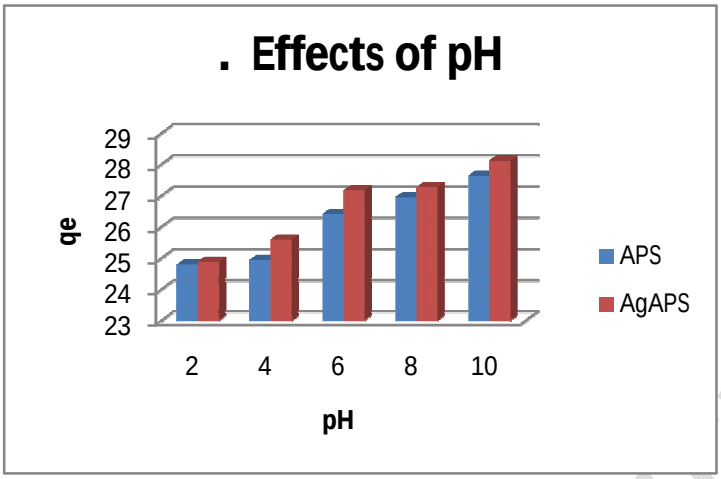

Figure 7. Effects of pH on the adsorption of copper onto avocado pear seed

3.6 Effect of Dosage on the Adsorption of Copper onto Avocado pear seed

One more significant and powerful factor influencing the adsorption process is the dosage of the adsorbent. Figure below shows the outcomes of the impacts of adsorbent dosage on copper adsorption onto APS and AgAPS. For APS and AgAPS, respectively, an increase in percentage removal between (88.0483 – 94.1900%) and (90.5850 – 95.3252%) was noted as the adsorbent dose increased from 0.1g to 0.5g. This could be explained by both the presence of active adsorption sites and a larger surface area. Nevertheless, the opposite pattern was noted, as seen in the figure below, which illustrates how the adsorbent dose increased along with a reduction in adsorption capacity.

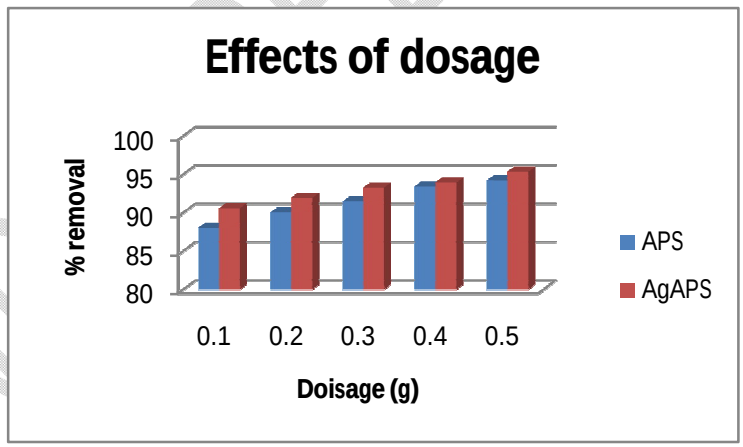

Figure .8. Effects of dosage on the percentage removal of copper onto avocado pear seed

3.7 Effect of Temperature on the Adsorption of Copper onto Avocado Pear Seed

The majority of contaminants' absorption from solution is also significantly influenced by the temperature of the effluent. In this context, the Figure below presents the findings of the investigation into the effects of temperature on Copper adsorption onto APS and AgAPS. The elimination of copper ions rose from 26.4145 mg/g to 28.5790 mg/g for APS and from 27.1756 mg/g to 28.9728 mg/g for AgAPS when the

temperature was raised from 303 to 323 K. This suggested that the reaction process is endothermic and that higher temperatures favor the adsorption of copper ions onto both adsorbents[26].The increase in the adsorption capacity may be as a result of the enhanced mobility of copper molecules with higher temperature for more interaction with the active sites of the adsorbent[19]. It is also attributed to the creation of new active sites on the adsorbent surface, due to the removal of some surface impurities as the temperature increases[19].

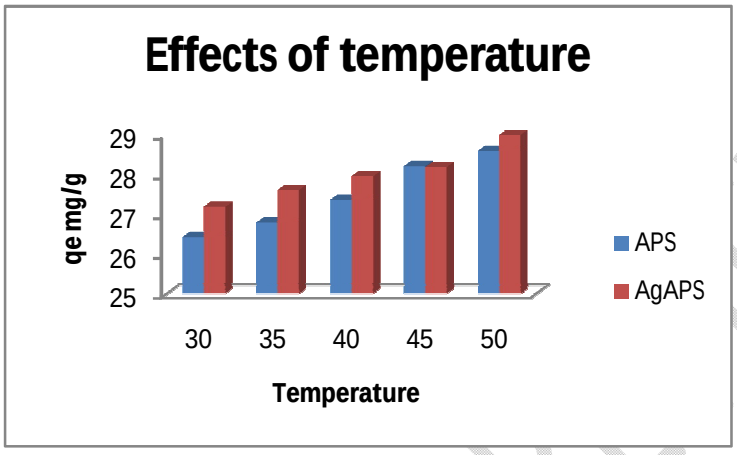

Figure 9. Effects of temperature on the adsorption of copper onto avocado pear seed

3.8 Kinetics of Copper adsorption onto Avocado Pear Seed

To explain the adsorption of copper onto APS and AgAPS, the experimental data were treated with pseudo first order kinetic model, pseudo second order kinetic model and intra-particle diffusion kinetic model. Plots for pseudo first order and pseudo second order kinetic models were presented respectively. The values of coefficient of determination R^2 for the pseudo second order model (0.999 and 0.999) fare higher than the pseudo first order model (0.904 and 0.890) for AgAPS and APS respectively, and also the estimated qe values from the pseudo second model were closer to the experimental values than the pseudo first order model. The goodness of fit and accurate prediction of qe both indicate that the pseudo second order model better describes the adsorption of copper onto APS and AgAPS and that chemisorptions is the likely mechanism of attraction [26]. A similar result was obtained in the adsorption of malachite green onto rattan saw dust[27].Copper and other metal ions in solution can be transported from the aqueous phase to the surface of the adsorbent, and can as well diffuse into the interior of the porous particles[24]. It is expected that the plot of qe versus $t^{1/2}$ would give a linear relationship when intraparticle diffusion is involved in the mechanism of the biosorption process and that intraparticle diffusion would be then controlling mechanism if the line passed through the origin[28]. However, for the case where the plots do not pass through the origin, the reason has been suggested that intra-particle diffusion is not the only mechanism involved in the sorption process due to some degree of boundary layer control[29]. The intercept of the intra-particle diffusion model (25.55 and 24.81) for AgAPS and APS respectively, indicated that copper adsorption onto APS and AgAPS is by surface reaction and diffusion into the pores of the materials. This is in agreement with results from[30;26].

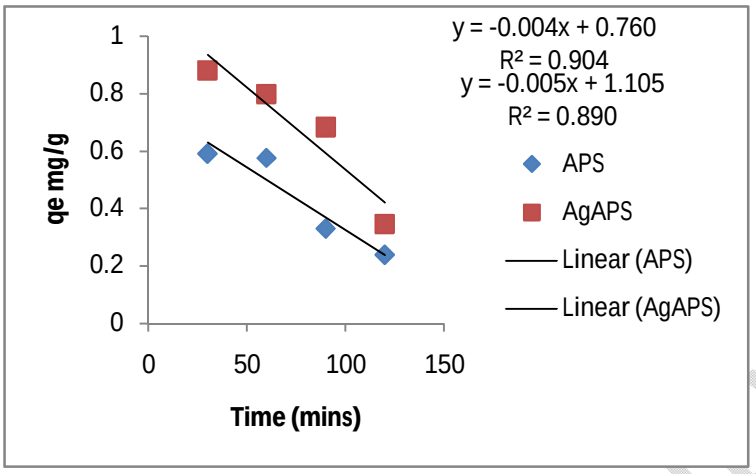

Fig 10 Pseudo first order kinetic plot for the adsorption of copper onto avocado pear seed

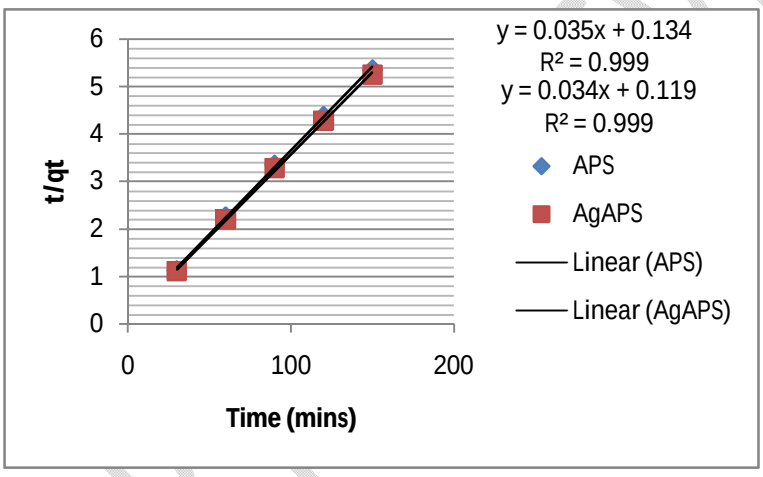

Fig 11Pseudo second order kinetic plot for the adsorption of copper onto avocado pear seed

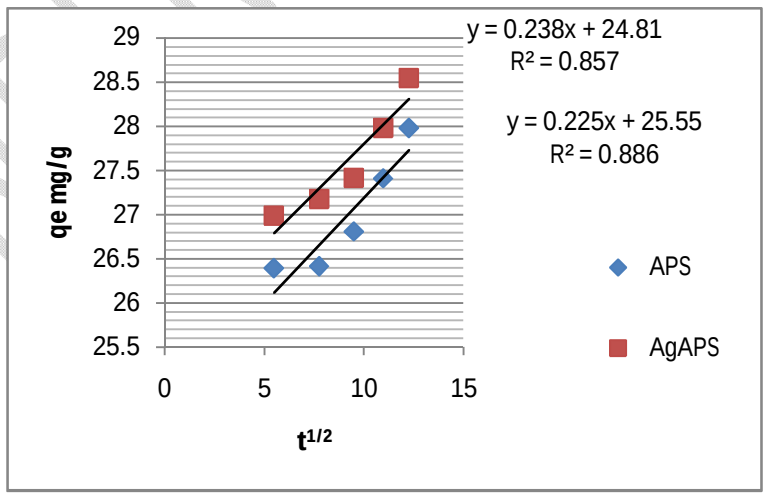

Figure 12. Intra-particle diffusion plot for the adsorption of copper onto avocado pear seed

3.9 Thermodynamics of Adsorption of Copper onto Avocado Pear Seed

The thermodynamic parameters; ΔH^o, ΔS^o and ΔG^o provides a very useful information on heat changes, spontaneity and randomness of the sorption process. The plot of lnK against temperature are presented in Figure 13 and the calculated thermodynamic parameters for the sorption of copper onto APS and AgAPS are presented below

Table 2. Thermodynamic parameters for the sorption of copper onto APS and AgAPS

	Cu APS	Ag APS
ΔH^0	0.4323	0.3991
ΔS^0	117.0611	105.0058
R^2	0.965	0.888
ΔG^0 303	-35,469.081	-31,816.358
308	-36,054.387	-32,341.387
313	-36,639.692	-32,886.416
318	-37,224.998	-33,391.445
323	-37,810.303	-33,916,474

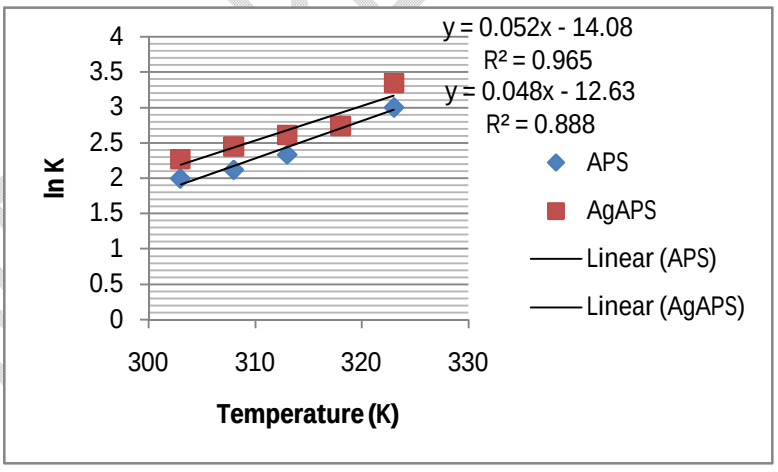

Fig 13 Thermodynamic plot for the adsorption of copper onto avocado pear seed

The positive value of ΔH^o values recorded for both APS and AgAPS indicated an exothermic removal of copper by APS and AgAPS, which correlates the increase in copper adsorption with temperature increase. The positive value of ΔS^o represents enhanced entropy on the solid-solution interface during the adsorption and development of structural changes, and thus irreversibility of the process[31]. The

negative values of Gibbs free energy in all the temperatures studied, represents the spontaneity of the process[31]. Elevation in ΔG^{o}, with temperature enhances the extent of adsorption and at higher temperatures the metal ion becomes hydrated faster and its adsorption increases.

4.0 CONCLUSION

It was discovered that the copper ions in industrial waste water can be adsorbed by biosynthesized silver metal nanocomposite made from avocado peer seed. Atomic Absorption Spectroscopy (AAS) was used to investigate the equilibrium kinetics and thermodynamics for the removal of heavy metals utilizing the bio-synthesized nanocomposites. FTIR, XRD, and SEM were used to characterize the silver metal nanocomposite that were biosynthesized. For the sorption of heavy metals, equilibrium and kinetic models were created by taking into account the effects of dosage, temperature, initial pH, contact time, and initial concentrations of heavy metal ions. Avocado raw seed absorbed copper ions, but its silver metal nanocomposite increased the amount of adsorption. In comparison to the raw agricultural wastes, the action of the adsorbent did demonstrate increased adsorption for the nanoparticles.The maximum percentage removal of copper ion was 92.2726% and 94.1900% for APS and AgAPS respectively.

Disclaimer (Artificial intelligence)

Option 1:

Author(s) hereby declare that NO generative AI technologies such as Large Language Models (ChatGPT, COPILOT, etc.) and text-to-image generators have been used during the writing or editing of this manuscript.

Option 2:

Author(s) hereby declare that generative AI technologies such as Large Language Models, etc. have been used during the writing or editing of manuscripts. This explanation will include the name, version, model, and source of the generative AI technology and as well as all input prompts provided to the generative AI technology

Details of the AI usage are given below:

1.

2.

3.

REFERENCES

1. Laurent, S., Forge, D., Port, M., Roch, A., Robic, C., Vander Elst,L., and Muller, R.N., (2010), Magnetic iron oxide nanoparticles: synthesis, stabilization, vectorization, physicochemical characterizations, and biological applications. Chem. Rev. 110.https://doi.org/10.1021/cr068445e.
2. Dreaden, E.C., Alkilany, A.M., Huang, X., Murphy, C.J. and El-Sayed, M.A., (2012), The golden age: gold nanoparticles for biomedicine. Chem. Soc. Rev. 41, 2740–2779.https://doi.org/10.1039/c1cs15237h.
3. Zuorro, A.; Iannone, A.; Natali, S and Lavecchia, R. (2019). Green Synthesis of Silver Nanoparticles Using Bilberry and Red Currant Waste Extracts. *Processes*, 7, 193.
4. Singh, N.B., Nagpal, G.; Agrawal, S and Rachna. (2018). Water purification by using Adsorbents: A Review. *Environmental Technology and Innovation,* 11, 187-240. DOI:https://doi.org/10.1016/j.eti.2018.05.006.
5. Khan, F., Shariq, M., Asif, M., Siddiqui, M., Malan, P and Ahmad, F. (2022). Green Nanotechnology: Plant-Mediated Nanoparticle Synthesis and Application. *Nanomaterials,* 12. DOI:https://doi.org/10.3390/nano12040673.
6. Adeyemi, O.O., Okpo, S.O., and Ogunti, O.O.,(2002). Analgesic and anti-inflammatory effects of the aqueous extract of leaves of Perseaamericana Mill (Lauraceae). *Fitoterapia.* 73(5):375–380. https://doi.org/10.1016/S0367-326X(02)00120-4.
7. Anaka, O. N., Ozolua, R. I., &Okpo, S. O. (2009). Effects of the aqueous seed extract of Perseaamericana Mill (Lauraceae) on the blood pressure of Sprague-Dawley rats. African Journal of Pharmacy and Pharmacology, 3(10), 485–490.
8. Ojewole, J. A., &Amabeoku, G. J. (2006). Anticonvulsant effect of Perseaamericana Mill. (Lauraceae) (Avocado) leaf aqueous extract in mice. Phytotherapy Research, 20(8), 696–700. https://doi.org/10.1002/ptr.1930.
9. Egbuonu, A. C. C., Cpara, C. I., &Atasie, O. C. (2017). Vitamins composition and antioxidant properties in normal and monosodium glutamate-compromised rats' serum of avocado pear (Perseaamericana) seed. Open Access Journal of Chemistry, 1(1), 19–24.
10. Alhassan, A. J., Sule, M. S., &Atiku, M. K. (2012). Effects of aqueous avocado pear (Perseaamericana) seed extract on alloxan-induced diabetes rats. Greener Journal of Medical Sciences, 2(1), 5–11.
11. Zaimee, M.Z.A.; Sarjadi, M.S and Rahman, M.L. (2021). Heavy Metals Removal from Water by Efficient Adsorbents. *Water*, 13:2659. DOI: https://doi.org/10.3390/w13192659.
12. Chowdhary, P., Bharagava, R. N., Mishra, S and Khan, N. (2020). Role of Industries in Water Scarcity and its Adverse Effects on Environment and Human Health. Environ. *Concerns Sustain. Dev.,* 235–256. DOI:10.1007/978-981-13-5889-0_12
13. Dahiya, S., Tripathi, R. M., &Hegde, A. G. (2008). Biosorption of lead and copper from aqueous solutions by pretreated crab and arca shell biomass. Bioresource Technology, 99(1), 179–187. https://doi.org/10.1016/j.biortech.2006.12.031.

14. Huang, W., & Li, Z. M. (2013). Removal of chromium(VI) from aqueous solution using activated carbon modified with nitric acid: thermodynamic and kinetic studies. Colloids and Surfaces B: Biointerfaces, 105, 113–119. https://doi.org/10.1016/j.colsurfb.2012.12.008.

15. Hua, M., Zhang, S., Pan, B., Zhang, W., Lv, L., & Zhang, Q. (2012). Heavy metal removal from water/wastewater by nanosized metal oxides: a review. Journal of Hazardous Materials, 211–212, 317–331. https://doi.org/10.1016/j.jhazmat.2011.10.016.

16. Esumi, K., Tano, T., Torigoe, K., & Meguro, K. (1990). Preparation and characterization of bimetallic Pd–Cu colloids by thermal decomposition of their acetate compounds in organic solvents. Journal of the Chemical Society, Faraday Transactions, 86(9), 1453–1459. https://doi.org/10.1039/FT9908601453.

17. Pileni, M. P. (2000). Fabrication and physical properties of self-organized silver nanocrystals. Pure and Applied Chemistry, 72(1–2), 53–65. https://doi.org/10.1351/pac200072010053.

18. Liz-Marzán, L. M., &Lado-Touriño, I. (1996). Reduction and stabilization of silver nanoparticles in ethanol by nonionic surfactants. Langmuir, 12(15), 3585–3589. https://doi.org/10.1021/la950618a.

19. Akpomie, K. G., &Conradie, J. (2020). Biogenic and chemically synthesized Solanumtuberosum peel–silver nanoparticle hybrid for the ultrasonic aided adsorption of bromophenol blue dye. Scientific Reports, 10, 17094. https://doi.org/10.1038/s41598-020-74254-y.
20. Dai, H., Huang, Y., Zhary, H., Ma, L., Huary, H., Wu, J., & Zhang, Y. (2020). Direct fabrication of hierarchically processed pineapple peel hydrogels for efficient conjugated adsorption. Carbohydrate Polymers, 280, 115599. https://doi.org/10.1016/j.carbpol.2021.115599.
21. He, Y., Wei, F., Ma, Z., Zhang, H., Yang, Q., Yao, B., Huang, Z., Li, J., Zeng, C., & Zhang, Q. (2017). Green synthesis of silver nanoparticles using seed extract of Alpinia katsumadai and their antioxidant, cytotoxicity, and antibacterial activities. RSC Advances, 7(39642–39651). https://doi.org/10.1039/C7RA05286C.
22. Chukwuemeka-Okorie, H. O., Ani, J. U., Agbo, S. U., Odewole, O. A., Ojo, F. K., Alum, O. L., Akpomie, K. G., Ofomatah, A. C., &Aralu, C. C. (2023). Adsorptive performance of green synthesized zinc oxide nanoparticles for the removal of cadmium (II) and lead (II) ions. IOP Conference Series: Earth and Environmental Science, 1178(1), 012021. https://doi.org/10.1088/1755-1315/1178/1/012021.
23. Dawodu, F. A., &Akpomie, K. G. (2014). Simultaneous adsorption of Ni(II) and Mn(II) ions from aqueous solution onto Nigerian Kaolinite clay. Journal of Materials Research and Technology, 3(2), 129–141.
24. Nwadiogbu, J. O., Okoye, P. A. C., Ajiwe, V. I. E., &Nnaji, J. N. (2016). Removal of crude oil from aqueous medium by sorption on hydrophobic corncobs: Equilibrium and kinetic studies. Journal of Taibah University for Science, 10(1), 56–63. https://doi.org/10.1016/j.jtusci.2015.03.014.
25. Hussain, J. I., Kumar, S., Hashmi, A. A., & Khan, Z. (2011). Silver nanoparticles: Preparation, characterization, and kinetics. *Advanced Materials Letters*, 2(3), 188–194. https://doi.org/10.5185/amlett.2011.1206.
26. Akpomie, K. G., &Conradie, J. (2020). Efficient synthesis of magnetic nanoparticle-Musa acuminata peel composite for the adsorption of anionic dye. Arabian Journal of Chemistry, 13(9), 7115–7131. https://doi.org/10.1016/j.arabjc.2020.07.017.

27. Hameed, B. H., & El-Khaiary, M. I. (2008). Malachite green adsorption by rattan sawdust: Isotherm, kinetic and mechanism modeling. Journal of Hazardous Materials, 159(2–3), 574–579. https://doi.org/10.1016/j.jhazmat.2008.02.054.
28. Igwe, J. C., &Abia, A. A. (2006). A bioseparation process for removing heavy metals from wastewater using biosorbents. African Journal of Biotechnology, 5(12), 1167–1179.
29. Bulut, E., Özacar, M., &Şengil, İ. A. (2008). Adsorption of malachite green onto bentonite: Equilibrium and kinetic studies and process design. Microporous and Mesoporous Materials, 115(3), 234–246. https://doi.org/10.1016/j.micromeso.2008.01.039.
30. Rahdar, S., Rahdar, A., Zafar, M. N., Shafqat, S. S., &Ahmadi, S. (2019). Synthesis and characterization of MgO supported Fe–Co–Mn nanoparticles with exceptionally high adsorption capacity for Rhodamine B dye. Journal of Materials Research and Technology, 8(5), 3800–3810. https://doi.org/10.1016/j.jmrt.2019.06.041.
31. Rahdar, S., Rahdar, A., Zafar, M. N., Shafqat, S. S., &Ahmadi, S. (2019). Synthesis and characterization of MgO supported Fe–Co–Mn nanoparticles with exceptionally high adsorption capacity for Rhodamine B dye. Journal of Materials Research and Technology, 8(5), 3800–3810. https://doi.org/10.1016/j.jmrt.2019.06.041